Hybrid Logical-Physical Qubit Interaction as a Post Selection Oracle

Nadav Carmel* and Nadav Katz†
The Hebrew University of Jerusalem

(Dated: May 26, 2023)

We demonstrate a property of the quantum 5-qubit stabilizer code that enables the interaction between qubits of different logical layers, and conduct a full density-matrix simulation of an interaction between a logical and a physical qubit. We use the logical qubit as an ancilla and find under which circumstances it gives an advantage over the bare physical ancilla approach, changing the circuit depth and noise level with decoherence processes at play. We use it as a post selection oracle for quantum phase estimation to detect errors propagating from the sensor qubit. Finally, we use our simulation to give noise thresholds both for computation and for sensing a signal using quantum phase estimation that are well within the capabilities of today's hardware.

In the field of quantum metrology, we are most interested in finding ways to recover the Heisenberg-limit scaling, promising that the error in estimating our observable scales as one over the number of measurements, probing time or number of probes [1]. Recent results indicate that this limit cannot be recovered in the presence of general Markovian noise if the Hamiltonian lies in the span of the noise operators [2–6]. Much effort has been made to recover the Heisenberg-limit scaling using quantum error correction [1, 3, 4, 7–13]. All these efforts focus on sequential quantum metrology, encoding the sensor as a logical qubit and using sophisticated methods to correct the errors while not correcting the signal itself.

Degen *et al.* [14] quantitatively defines the Dynamic Range of a non-entangled quantum sensor, and finds it scales as the square root of the measurement time due to shot noise. Algorithmic quantum sensing is crucial in extending the dynamic range of quantum sensors by assigning appropriate weights to different quantum measurements, thereby approaching the Heisenberg limit. Recently the use of algorithmic quantum sensing has caught the attention of the community [12, 15]. While Quantum Phase Estimation (QPE) is a prominent algorithmic sensing protocol it has various applications in other areas of study [16–20], the most famous one being Shor's algorithm. Thus extensive research has investigated the performance of QPE under noise [21–24]. Achieving the Heisenberg-limit scaling requires an unbiased probability distribution [5, 14]. However, decoherence introduces bias to the probability distribution obtained from QPE, hindering the attainment of the Heisenberg limit. In this letter, we propose a method to mitigate bias, thereby approaching the limit.

In algorithmic quantum sensing protocols, the presence of ancillas introduces a new realm to study wherein error correction or error detection is performed on the ancillas rather than the sensor itself. Making only the ancilla logical while letting the sensor remain a physical sensor, enforces the need of hybrid logical-physical interaction. While fault-tolerant [25] hybrid interaction could be pursued using methods such as flag fault-tolerance [26–30], for sensing purposes, a limited number of successful runs is sufficient. Applying post selection on the sensor has proved to be a vital tool for any experimental implementation of sensing [6, 24, 31–34]. It has been shown that the error in verified phase estimation [24], an error mitigation technique based on what we call sensor post-selection (SPS), scales as the squared probability for a single gate error p^2.

In this letter, we take advantage of error propagation from the sensor qubit to the logical ancilla qubit. We get rid of a larger portion of the noise by encoding some of it on the redundant degrees of freedom of the Hilbert space of the logical ancilla, applying only error detection and post-selecting the results. We use the simple 5-qubit code which has an interesting attribute: all errors with a weight smaller or equal to 2 cause a non-trivial syndrome. Thus if the probability of error in one ancilla in the whole algorithm is p, then the probability of error after logically post-selecting (LPS) is proportional to p^3. See [35] for the 5-qubit-code stabilizers and a syndrome-cause table.

Since any multi-qubit gate can be decomposed into single qubit gates and CNOT gates [36], our focus should be understanding how to implement the CNOT gate between logical and physical qubits, as control and target respectively. Some quantum error correction codes (QECC) have a useful parity attribute: The logical states, $|0\rangle_L$ and $|1\rangle_L$, are made up of a sum of quantum states with an even or odd number of 1's, respectively. One such code is the 5-qubit-code, with basis states defined in [35]. In the case of one logical layer, this attribute allows us to implement the CNOT gate in a semi-transversal manner, as in Fig. 1 (b). This can be generalized trivially for any number of logical layers, provided that the quantum code used for each layer has this attribute. See [35] for the logical gates necessary for the QPE algorithm using the 5-qubit code.

Throughout the letter a fidelity between a 6-qubit-state and a 2-qubit-state has been calculated. This has been done by taking the 6-qubit-state's density matrix ρ

* nadav.carmel1@huji.mail.ac.il
† nadav.katz@mail.huji.ac.il

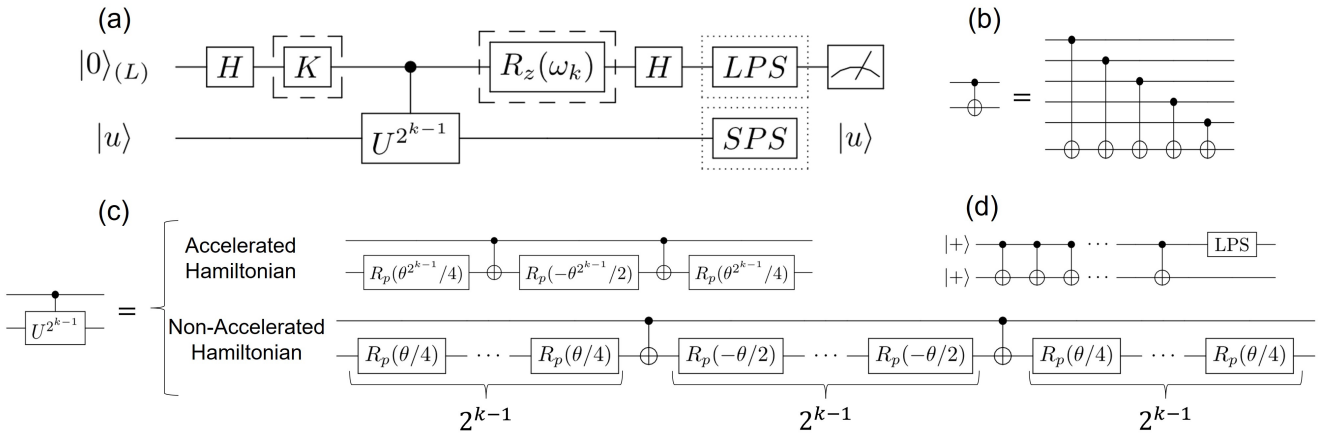

FIG. 1: Circuits used in this work. (a) Iterative versions of QPE. The dashed K gate appears only in Kitaev's iterative version, where K can be $K = S$ and $K = I$. The dashed R_z gate appears only in Iterative Phase Estimation Algorithm (IPEA), where the feedback angle depends on the previously measured bits through $\omega_k = -2\pi(0.0x_{k+1}x_{k+2}\dots x_m)$, and $\omega_m = 0$.. The dotted LPS (Logical Post Selection) and SPS (Sensor Post Selection) gates appear in circuits as described in the main text and other figures. (b) Logically controlled CNOT gate, with the first 5 qubits acting as a logical qubit and the sixth qubit as the target qubit, encoded one logical layer lower then the control. (c) The controlled operation in this work is a single qubit rotation gate where $p = x$ or $p = z$. In the figure are implementations of accelerated and non-accelerated controlled signal Hamiltonians. (d) The circuit used for exploring logical-physical interaction length, Fig. 2 (b).

and calculating the effective reduced density matrix ρ':

$$\rho' = \begin{pmatrix} \langle 0_L0|\rho|0_L0\rangle & \langle 0_L0|\rho|0_L1\rangle & \langle 0_L0|\rho|1_L0\rangle & \langle 0_L0|\rho|1_L0\rangle \\ \langle 0_L1|\rho|0_L0\rangle & \langle 0_L1|\rho|0_L1\rangle & \langle 0_L1|\rho|1_L0\rangle & \langle 0_L1|\rho|1_L0\rangle \\ \langle 1_L0|\rho|0_L0\rangle & \langle 1_L0|\rho|0_L1\rangle & \langle 1_L0|\rho|1_L0\rangle & \langle 1_L0|\rho|1_L0\rangle \\ \langle 1_L1|\rho|0_L0\rangle & \langle 1_L1|\rho|0_L1\rangle & \langle 1_L1|\rho|1_L0\rangle & \langle 1_L1|\rho|1_L0\rangle \end{pmatrix} \tag{1}$$

Note that this is not necessarily a pure state. Performing LPS in our simulation is done by projecting the state onto the code, forcing each stabilizer to measure '0' [35]. In addition, when we perform error correction and the resulting state is not within the code, the reduction operation of Eq. 1 is not trace preserving. Due to the projective nature of these operations, to calculate the fidelity or distance between two states, where one of them is not a pure density matrix, we save the trace of each one and normalize them before hand. We define the lost information [35] to be the fraction of information lost due to post selection, $l_i = 1 - Tr(\rho')$ where ρ' is the reduced 2-qubit density matrix defined in Eq.1. We quantify the noise by worst-case single gate fidelity, calculated by putting a qubit in it's most susceptible state to the applied noise - for example, the state $|+\rangle$ for dephasing and $|1\rangle$ for amplitude damping.

Quantum phase estimation encompasses a family of algorithms for estimating the unknown phase, denoted as ϕ, associated with the eigenvector $|u\rangle$ of a unitary operator U, having the eigenvalue $e^{2\pi i\phi}$. This estimation is achieved by employing black boxes capable of preparing the state $|u\rangle$ and performing controlled-U^{2^j} operations, where j is a positive integer. These controlled operations can be either accelerated or non-accelerated, where accelerated Hamiltonians have been extensively studied in the context of algorithmic complexity theory and super-resolution [37, 38]. Acceleration can be achieved through specialized techniques like angle-dependent magnetic field application or general methods like QAQC [39] and VFF [40].

The algorithm employs two quantum registers: one for the measured operator U and another for ancilla qubits needed for computation [41]. In this study, we consider two iterative versions of the algorithm depicted in Fig. 1(a) (dashed line alternatives), which utilize a single ancilla qubit for phase estimation. These versions are particularly valuable for Noisy Intermediate Scale Quantum (NISQ) computers, where simultaneous utilization of multiple qubits is limited. We utilize Kitaev's approach [35] with accelerated Hamiltonians, which is essentially equivalent to the shortest application of IPEA [35] in terms of fidelity. This approach allows us to average over measured phases and evaluate the performance of LPS (Fig. 2 (b,c)). For unaccelerated Hamiltonians, we simulate the case using IPEA (Figs. 2 (a,d), 3 (a-d)).

Each QPE application yields a probability distribution of all possible measurement results, derived from the probabilities of correctly measuring each digit during each iteration or ancilla qubit. Multiple measurements of each digit can be performed, followed by a majority vote, to enhance the probability of accurate measurements, as illustrated in Fig.2 (a). Decoherence introduces bias to this histogram, altering the mean and standard deviation, as illustrated in Fig.3.

Quantum phase estimation finds utility in both quantum computation and quantum metrology, with different

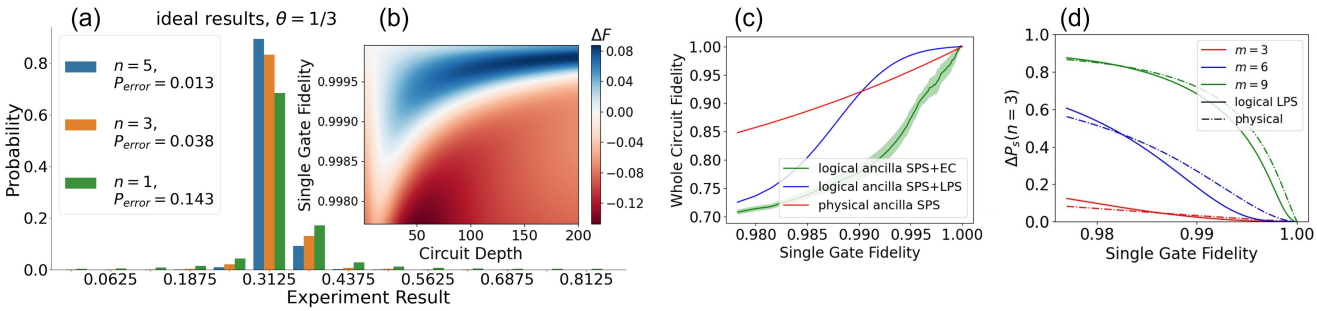

FIG. 2: Demonstrating the general properties of LPS gadget under different scenarios. (a) Estimating $\theta = 1/3$ up to 4 binary digits. The resulting probability distributions are obtained from IPEA by measuring each digit $n \in \{1, 3, 5\}$ times and taking a majority vote. (b) Mapping the thresholds of logical and physical control for noise level and circuit depth, simulating the circuit in Fig. 1d. Here all qubits are noisy (susceptible only to dephasing) in all stages of the circuit, including syndrome extraction. The white line is the location of the threshold, and blue/red areas are the fidelity difference at the end of the circuit $\Delta F = F_{logical} - F_{physical}$. A non-monotonic behaviour of the fidelity with circuit depth is observed. (c) Fidelity after an iteration of Kitaev's approach with accelerated sensing Hamiltonian averaged over 10 angles, with dephasing ancillas and a sensor in the ground state measuring $R_z(\theta)$. The red line represents physical ancilla with SPS, the blue line logical ancilla with SPS and LPS while the green line is logical ancilla with error correction right before the measurement. These graphs are for $K = I$ and similar graphs are available for $K = S$ in [35]. It is clear that there is a threshold in which using LPS outputs a state closer to the ideal, even when the noise resides in the ancillas alone. (d) Difference between the ideal success probability of IPEA and a noisy implementation, both for physical and logical ancillas, for $n = 3$. Here the ancillas are perfect and the sensor dephases from the $|+\rangle$ eigenstate of $R_x(\theta)$. The probabilities are extracted by summing the two binary results closest to the real measured angle, $2\pi/\sqrt{3}$.

requirements in each. In quantum computation, the focus is on the probability of success after a single algorithm application. In quantum metrology, the primary interest lies in measuring a value and its associated error with the Heisenberg scaling. In this study, we first assess the performance of the LPS gadget by measuring fidelity at the circuit's end and estimating the probability of a single-shot success in quantum phase estimation, disregarding any lost information (Fig.2). Subsequently, we evaluate the algorithm's performance in the context of algorithmic sensing, accounting for lost information, as demonstrated in Fig.3.

Our first result is on the general behaviour of logical-physical interaction and LPS. As mentioned earlier, multi-qubit interactions can be simplified to single qubit gates along with CNOT or CZ entangling gates. A crucial question arises regarding the threshold value at which logical control surpasses physical control, and its dependence on the number of entangling gates. To address this question, we consider infinite T_1 and varying T_2 values for all qubits. Additionally, we vary the number of CNOT gates within the range of [1, 200), as depicted in Fig.1 (d) (simulated circuit). We start with the initial eigenstate $|++\rangle$ of CNOT (the first qubit is the ancilla and the second is the sensor), which is highly susceptible to T_2 noise. The ancilla qubit is tested both as a logical 5-qubit or a bare physical qubit. After applying N_g CNOT gates, we subject the system to noisy LPS. We calculate and save the fidelity between the output state and $|++\rangle$ using Eq.1, subsequently generating a color map illustrating the fidelity difference between logical and physical control (Fig.2 (b)). The number of entangling gates serves as one axis, while the worst-case single gate fidelity serves as the other. It should be noted that we employ noisy syndrome extraction, resulting in a constant overhead of approximately 20 gates in circuit depth. As depicted, there exists a range of circuit depths and gate fidelities wherein logical control outperforms physical control. The specific values obtained in our work are contingent on simulation parameters and are expected to vary with different quantum hardware. Nonetheless, the overall structure of the dependence is expected to stay similar.

Our second result is on the fidelity at the end of a QPE iteration. Algorithmic quantum sensing utilizing the QPE algorithm is particularly effective when accelerated Hamiltonians are assumed, allowing for high-fidelity application of high powers of the time evolution operator. In this letter, we consider accelerated Hamiltonians implemented as shown in Fig.1 (c), simulating one iteration of Kitaev's approach (Fig.1(a)) with logical post-selection (LPS) and sensor post-selection (SPS). We calculate the fidelity, after post-selection, between the noisy implementation and the two-qubit ideal state immediately prior to measurement, thus assuming a perfect measurement.

The results, including the fidelity of the error-corrected state, are presented in Fig.2 (c). Notably, the error-corrected state exhibits stochastic behaviour, which is averaged in the figure due to its inherent randomness - a mistake in syndrome extraction leads to the application

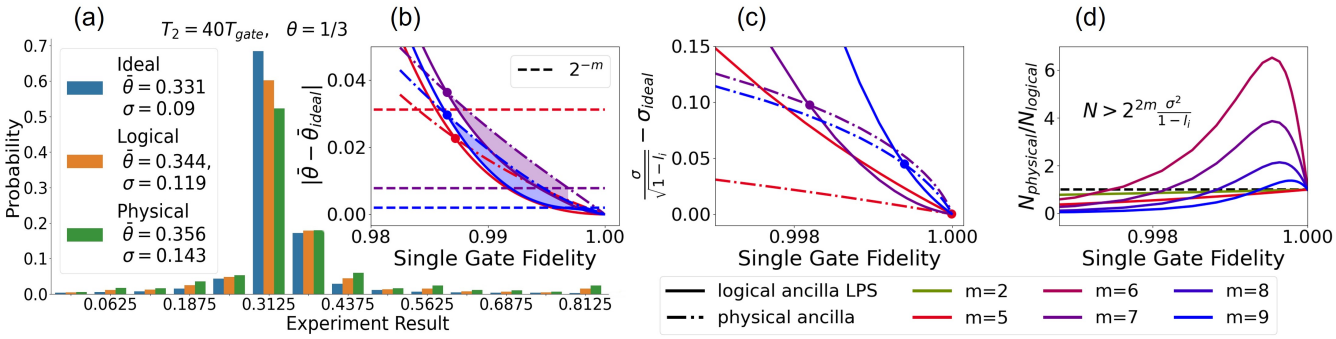

FIG. 3: Demonstrating LPS as a post selection oracle for IPEA (Fig.1a) in the context of quantum metrology. b-d are obtained by measuring $R_x(\frac{2\pi}{\sqrt{3}})$ on the $|+\rangle$ eigenstate, with a dephasing sensor and perfect ancillas. (a) Estimating $\theta = 1/3$ up to 4 binary digits. The resulting probability distributions are obtained from noisy IPEA algorithms as indicated in the figure. It is evident that LPS makes the probability distribution less biased, thus approaching the ideal and the Heisenberg limit. (b) Measuring the mean of the circular probability distribution of results for a number of desired precisions m. It is easy to see that there exists parameter regimes of deep circuits and approximately a minimum of 0.986 worst case single gate fidelity such that the logical control gives a better estimate of the mean. The shaded regions indicate on parameter regimes where it is beneficial to use LPS accuracy-wise. Lost information of the threshold is around 99%. (c) Statistical error in estimating the phase. (d) Ratio of the assessed minimum number of trials needed to reach digital accuracy by Eq.2. It is evident from (c,d) that up from approximately 0.997 worst case single gate fidelity we start observing an improvement of results in the sense of a lower sensing time, while lost information of the threshold is around 75%.

of a faulty correction operator, and it should be noted that we incorporate only one round of error correction in the circuit. Further details on the improved scaling of the error probability and complementary information can be found in [35].

Counter-intuitively, we observe a threshold at which logical control surpasses physical control. This is unexpected since only the ancillas are subject to noise. Apparently, there are scenarios in which employing five noisy ancillas outperforms using only one noisy ancilla. Strikingly, the obtained thresholds fall within the capabilities of today's state-of-the-art technology! [42].

As mentioned earlier, it is sometimes advantageous to measure each digit multiple times and employ majority voting to enhance the success probability. In the NISQ era, we assume utilizing the deepest possible circuit for accurate phase measurement, where at most two possible results contribute to the algorithm's success probability (Fig.2(d)). For an extended discussion on the success probability please refer to [35]. It is evident that by acting as a post selecting oracle the LPS gadget increased the probability of success after a single run for a wide range of parameters.

In quantum metrology, the precision and statistical error of measurements are of utmost importance. Our previous findings demonstrate that the LPS gadget in deep quantum circuits has the potential to mitigate bias in the resulting probability distribution, leading us to give up on the non-trivial the assumption of accelerated Hamiltonians. Instead, we employ the Iterative Phase Estimation Algorithm (IPEA) with LPS and without SPS (Fig.1(a)). Specifically, we select the irrational phase $\phi = 2\pi/\sqrt{3}$ and evaluate it up to nine binary digits of accuracy, necessitating approximately $3 * 2^8 \approx 800$ consecutive gate applications, including syndrome extraction. We compute the mean $\bar{\theta}$ and standard deviation σ of the resulting circular probability distribution (due to the phase's periodicity).

By averaging a Gaussian-like distribution [16], the error scaling of the mean is determined to be $1/\sqrt{n}$, where n represents the number of post-selected trials. The total measurement error is defined as the maximum between the digital error 2^{-m} (with m denoting the desired precision) and the statistical error approximated in the limit of large n by $\sigma/\sqrt{N(1-l_i)}$, where N corresponds to the total number of algorithm trials. We define the minimal number of trials needed for the statistical error to reach to the digital error to be

$$N_{min} = 2^{2m}\frac{\sigma^2}{1-l_i} \tag{2}$$

We anticipate the most significant improvement in the realistic case of a noisy sensor and perfect ancillas. Specifically, we initialize the sensor in the eigenstate $|+\rangle$ and measure the operator $R_x(\frac{2\pi}{\sqrt{3}})$ while assuming perfect ancillas and allowing only dephasing to occur to the sensor. The results, presented in Fig. 3, demonstrate that even in the limit of infinite measurements, utilizing the LPS gadget enhances the accuracy of the mean compared to the ideal scenario (without noise). This improvement continues until the physical control method achieves the desired digital accuracy. Notably, Fig. 3(c-d) reveals the existence of noise thresholds, indicating substantial improvements of up to an order of magnitude in error

estimation and in the total number of experiments when comparing physical and logical control. Supplementary results can be found in [35].

In conclusion, we have introduced the concept of logical-physical qubit interaction. We have identified a parameter regime where its utilization is advantageous, considering circuit depth and worst case single gate fidelity, particularly in the presence of dephasing as the primary source of error [21, 43]. By encoding noise into a larger Hilbert space and employing post selection of purified states, we have demonstrated improvements of up to an order of magnitude in algorithmic quantum sensing within various real-world sensing scenarios. Logical post selection has proven to be effective in cases where ancilla qubits are more resilient to noise compared to the sensor or when Hamiltonian fast-forwarding is possible. The hybrid logical-physical interaction has considerable applications in further research: it can be efficient in algorithms that require long-lived ancilla qubits like state distillation, error mitigation and algorithmic sensing [44–46]. However, the drawback of information loss due to post selection should be noted, and recent studies are exploring methods for simulating without the need for post selection [47]. This concept of LPS opens up new frontiers, such as designing entangling gates between a logical qubit and a physical qubit with minimum error or error propagation, potentially leveraging fault-tolerant flag techniques[26–30]. Our work showcases the suitability of the five qubit code for enabling this type of interaction and we believe that it can also be implemented with today's most promising codes, such as the surface codes [48].

We acknowledge T.Gefen and A.Retzker for fruitful discussions.

[1] S. Zhou, C. L. Zou, and L. Jiang, Saturating the quantum Cramér-Rao bound using LOCC, Quantum Science and Technology **5**, 36 (2020), arXiv:1809.06017.

[2] S. Zhou, M. Zhang, J. Preskill, and L. Jiang, Achieving the Heisenberg limit in quantum metrology using quantum error correction, *Nature Communications* **9**, 10.1038/s41467-017-02510-3 (2018), arXiv:1706.02445.

[3] D. Layden and P. Cappellaro, Spatial noise filtering through error correction for quantum sensing, npj Quantum Information **4**, 10.1038/s41534-018-0082-2 (2018), arXiv:1708.06729.

[4] I. Rojkov, D. Layden, P. Cappellaro, J. Home, and F. Reiter, Bias in Error-Corrected Quantum Sensing, Physical Review Letters **128**, 1 (2022), arXiv:2101.05817.

[5] C. Chen, P. Wang, and R. B. Liu, Effects of local decoherence on quantum critical metrology, Physical Review A **104**, 10.1103/PhysRevA.104.L020601 (2021), arXiv:2008.04879.

[6] Y. Matsuzaki and S. Benjamin, Magnetic-field sensing with quantum error detection under the effect of energy relaxation, Physical Review A **95**, 1 (2017), arXiv:1611.10264.

[7] Z. Ma, P. Gokhale, T. X. Zheng, S. Zhou, X. Yu, L. Jiang, P. Maurer, and F. T. Chong, Adaptive Circuit Learning for Quantum Metrology, Proceedings - 2021 IEEE International Conference on Quantum Computing and Engineering, QCE 2021 , 419 (2021), arXiv:2010.08702.

[8] F. Reiter, A. S. Sørensen, P. Zoller, and C. A. Muschik, Dissipative quantum error correction and application to quantum sensing with trapped ions, Nature Communications **8**, 10.1038/s41467-017-01895-5 (2017).

[9] D. A. Herrera-Martí, T. Gefen, D. Aharonov, N. Katz, and A. Retzker, Quantum Error-Correction-Enhanced Magnetometer Overcoming the Limit Imposed by Relaxation 10.1103/PhysRevLett.115.200501 (2014), arXiv:1410.7556.

[10] G. Arrad, Y. Vinkler, D. Aharonov, and A. Retzker, Increasing sensing resolution with error correction 10.1103/PhysRevLett.112.150801 (2013), arXiv:1310.3016.

[11] T. Unden, P. Balasubramanian, D. Louzon, Y. Vinkler, M. B. Plenio, M. Markham, D. Twitchen, I. Lovchinsky, A. O. Sushkov, M. D. Lukin, A. Retzker, B. Naydenov, L. P. Mcguinness, and F. Jelezko, Quantum metrology enhanced by repetitive quantum error correction, .

[12] T. Kapourniotis and A. Datta, Fault-tolerant quantum metrology, Physical Review A **100**, 10.1103/PhysRevA.100.022335 (2019), arXiv:1807.04267.

[13] Q. Zhuang, J. Preskill, and L. Jiang, Distributed quantum sensing enhanced by continuous-variable error correction, New Journal of Physics **22**, 1 (2020), arXiv:1910.14156.

[14] C. L. Degen, F. Reinhard, and P. Cappellaro, Quantum sensing 10.1103/RevModPhys.89.035002 (2016), arXiv:1611.02427.

[15] M. Takita, K. Inoue, S. Lekuch, Z. K. Minev, J. M. Chow, and J. M. Gambetta, Exploiting dynamic quantum circuits in a quantum algorithm with superconducting qubits, (2021), arXiv:arXiv:2102.01682v1.

[16] T. E. O'Brien, B. Tarasinski, and B. M. Terhal, Quantum phase estimation of multiple eigenvalues for small-scale (noisy) experiments 10.1088/1367-2630/aafb8e (2018), arXiv:1809.09697.

[17] P. M. Q. Cruz, G. Catarina, and R. Gautier, Optimizing quantum phase estimation for the simulation of Hamiltonian eigenstates, , 1 (2020), arXiv:arXiv:1910.06265v2.

[18] R. Santagati, J. Wang, A. A. Gentile, S. Paesani, N. Wiebe, J. R. Mcclean, P. J. Shadbolt, D. Bonneau, J. W. Silverstone, D. P. Tew, X. Zhou, and M. G. Thompson, Witnessing eigenstates for quantum simulation of Hamiltonian spectra, arXiv:arXiv:1611.03511v5.

[19] S. Kais, A Universal Quantum Circuit Scheme For Finding Complex Eigenvalues, arXiv:arXiv:1302.0579v5.

[20] J. Tilly, H. Chen, S. Cao, D. Picozzi, K. Setia, Y. Li, E. Grant, L. Wossnig, I. Rungger, G. H. Booth, and J. Tennyson, *Physics Reports*, Vol. 986 (2022) pp. 1–128, arXiv:2111.05176.

[21] F. Chapeau-Blondeau and E. Belin, Fourier-transform quantum phase estimation with quantum phase noise, Signal Processing **170**, 1 (2020).

[22] M. Dobšíček, G. Johansson, V. Shumeiko, and G. Wendin, Arbitrary accuracy iterative quantum phase

estimation algorithm using a single ancillary qubit: A two-qubit benchmark, Physical Review A - Atomic, Molecular, and Optical Physics **76**, 10.1103/PhysRevA.76.030306 (2007).

[23] I. Garc and D. L. Shepelyansky, Quantum phase estimation algorithm in presence of static imperfections, (2007), arXiv:arXiv:0711.1756v1.

[24] T. E. O'Brien, S. Polla, N. C. Rubin, W. J. Huggins, S. McArdle, S. Boixo, J. R. McClean, and R. Babbush, Error Mitigation via Verified Phase Estimation, PRX Quantum **2**, 1 (2021), arXiv:2010.02538.

[25] D. Aharonov and M. Ben-or, Fault-tolerant quantum computation with constant error rate, , 1 (1997), arXiv:9906129v1 [arXiv:quant-ph].

[26] R. Chao and B. W. Reichardt, Fault-tolerant quantum computation with few qubits 10.1038/s41534-018-0085-z (2017), arXiv:1705.05365.

[27] T. Tansuwannont, C. Chamberland, and D. Leung, Flag fault-tolerant error correction, measurement, and quantum computation for cyclic CSS codes 10.1103/PhysRevA.101.012342 (2018), arXiv:1803.09758.

[28] R. Chao and B. W. Reichardt, Flag fault-tolerant error correction for any stabilizer code 10.1103/PRXQuantum.1.010302 (2019), arXiv:1912.09549.

[29] B. W. Reichardt, Fault-tolerant quantum error correction for Steane's seven-qubit color code with few or no extra qubits 10.1088/2058-9565/abc6f4 (2018), arXiv:1804.06995.

[30] D. M. Debroy and K. R. Brown, Extended flag gadgets for low-overhead circuit verification, Physical Review A **102**, 1 (2020), arXiv:2009.07752.

[31] B. M. Varbanov, F. Battistel, B. M. Tarasinski, V. P. Ostroukh, T. E. O'Brien, L. DiCarlo, and B. M. Terhal, Leakage detection for a transmon-based surface code, npj Quantum Information **6**, 1 (2020), arXiv:2002.07119.

[32] H. Kwon, C. Oh, Y. Lim, H. Jeong, and L. Jiang, Efficacy of virtual purification-based error mitigation on quantum metrology, , 1 (2023), arXiv:2303.15838.

[33] K. Yamamoto, S. Endo, H. Hakoshima, Y. Matsuzaki, and Y. Tokunaga, Error-Mitigated Quantum Metrology via Virtual Purification, Physical Review Letters **129**, 10.1103/PhysRevLett.129.250503 (2022), arXiv:2112.01850.

[34] D. R. Arvidsson-Shukur, N. Yunger Halpern, H. V. Lepage, A. A. Lasek, C. H. Barnes, and S. Lloyd, Quantum advantage in postselected metrology, Nature Communications **11**, 1 (2020), arXiv:1903.02563.

[35] See supplemental material at [url], .

[36] M. A. Nielsen and I. L. Chuang, *Quantum computation and quantum information* (Cambridge University Press, 2010) p. 676.

[37] Y. Atia and D. Aharonov, Fast-forwarding of Hamiltonians and exponentially precise measurements, Nature Communications **8**, 1 (2017), arXiv:1610.09619.

[38] Y. Aharonov and S. Popescu, Measuring Energy, Estimating Hamiltonians, and the Time-Energy Uncertainty Relation, (2002).

[39] S. Khatri, R. LaRose, A. Poremba, L. Cincio, A. T. Sornborger, and P. J. Coles, Quantum-assisted quantum compiling 10.22331/q-2019-05-13-140 (2018), arXiv:1807.00800.

[40] C. Cîrstoiu, Z. Holmes, J. Iosue, L. Cincio, P. J. Coles, and A. Sornborger, Variational fast forwarding for quantum simulation beyond the coherence time, npj Quantum Information **6**, 10.1038/s41534-020-00302-0 (2020), arXiv:1910.04292.

[41] A. Y. Kitaev, Quantum measurements and the Abelian Stabilizer Problem, , 1 (1995), arXiv:9511026 [quant-ph].

[42] A. Kandala, K. X. Wei, S. Srinivasan, E. Magesan, S. Carnevale, G. A. Keefe, D. Klaus, O. Dial, and D. C. McKay, Demonstration of a High-Fidelity CNOT for Fixed-Frequency Transmons with Engineered ZZ Suppression, (2020), arXiv:2011.07050.

[43] A. Yu and A. Y. Chernyavskiy, On the fidelity of quantum gates under T1 and T2 relaxation 10.1117/12.2522383 (2021).

[44] P. Czarnik, A. Arrasmith, L. Cincio, and P. J. Coles, Qubit-efficient exponential suppression of errors, arXiv:arXiv:2102.06056v2.

[45] C. Piveteau, D. Sutter, S. Bravyi, J. M. Gambetta, and K. Temme, Error Mitigation for Universal Gates on Encoded Qubits, Physical Review Letters **127**, 10.1103/PhysRevLett.127.200505 (2021), arXiv:2103.04915.

[46] W. J. Huggins, S. McArdle, T. E. O'Brien, J. Lee, N. C. Rubin, S. Boixo, K. B. Whaley, R. Babbush, and J. R. McClean, Virtual Distillation for Quantum Error Mitigation, Physical Review X **11**, 1 (2021), arXiv:2011.07064.

[47] M. Ippoliti and V. Khemani, Postselection-Free Entanglement Dynamics via Spacetime Duality, Physical Review Letters **126**, 10.1103/PhysRevLett.126.060501 (2021), arXiv:2010.15840.

[48] E. Dennis, A. Kitaev, A. Landahl, and J. Preskill, Topological quantum memory, Journal of Mathematical Physics **43**, 4452 (2002), arXiv:0110143 [quant-ph].

[49] H. Ahmadi and C.-F. Chiang, Quantum Phase Estimation with Arbitrary Constant-precision Phase Shift Operators, (2010), arXiv:1012.4727.

[50] S. Cheng, C. Cao, C. Zhang, Y. Liu, S.-Y. Hou, P. Xu, and B. Zeng, Simulating Noisy Quantum Circuits with Matrix Product Density Operators 10.1103/PhysRevResearch.3.023005 (2020), arXiv:2004.02388.

[51] T. J. Yoder, R. Takagi, and I. L. Chuang, Universal fault-tolerant gates on concatenated stabilizer codes, Physical Review X **6**, 10.1103/PhysRevX.6.031039 (2016), arXiv:1603.03948.

[52] S. Johnstun and J.-F. Van Huele, Optimizing the Phase Estimation Algorithm Applied to the Quantum Simulation of Heisenberg-Type Hamiltonians, (2021), arXiv:2105.05018.

[53] K. Butler and M. Stephens, The Distribution of a Sum of Binomial Random Variables, (2016).

[54] S. Zhou, M. Zhang, J. Preskill, L. Jiang, N. Haven, and N. Haven, Achieving the Heisenberg limit in quantum metrology using quantum error cor- rection, arXiv:arXiv:1706.02445v2.

[55] I. García-Mata and D. L. Shepelyansky, Quantum phase estimation algorithm in presence of static imperfections, European Physical Journal D **47**, 151 (2008), arXiv:0711.1756.

[56] D. A. Steck and D. Steck, *Quantum and Atom Optics* (2019).